



Photon energy absorption and exposure buildup factors for deep penetration in human tissues

O. Kadri^{1,2} · A. Alfuraih¹

Received: 29 August 2019/Revised: 1 October 2019/Accepted: 13 October 2019/Published online: 15 November 2019
© China Science Publishing & Media Ltd. (Science Press), Shanghai Institute of Applied Physics, the Chinese Academy of Sciences, Chinese Nuclear Society and Springer Nature Singapore Pte Ltd. 2019

Abstract Using photons in therapeutic and diagnostic medicine requires accurate computation of their attenuation coefficients in human tissues. The buildup factor, a multiplicative coefficient quantifying the ratio of scattered to primary photons, measures the degree of violation of the Beer–Lambert law. In this study, the gamma-ray isotropic point source buildup factors, specifically, the energy absorption buildup factor (EABF) and exposure buildup factor, are estimated. The computational methods used include the geometric progression fitting method and simulation using the Geant4 (version 10.4) Monte Carlo simulation toolkit. The buildup factors of 30 human tissues were evaluated in an energy range of 0.015–15 MeV for penetration depths up to 100 mean free paths (mfp). At all penetration depths, it was observed that the EABF seems to be independent of the mfp at a photon energy of 1.5 MeV and also independent of the equivalent atomic number (Z_{eq}) in the photon energy range of 1.5–15 MeV. However, the

buildup factors were inversely proportional to Z_{eq} for energies below 1.5 MeV. Moreover, the Geant4 simulations of the EABF of water were in agreement with the available standard data. (The deviations were less than 5%.) The buildup factors evaluated in the present study could be useful for controlling human exposure to radiation.

Keywords Buildup factors · Human tissues · Geant4 · GP fitting · Gamma rays

1 Introduction

Gamma rays are used in medicine for therapy and diagnosis worldwide [1]. However, carelessness and poor knowledge of radiation safeguards can lead to death. Thus, an accurate investigation of the interaction of ionizing radiation with human tissues and organs is necessary to avoid this outcome. Ionizing radiation can biologically affect human tissues and organs depending on the absorbed energy, type of radiation (alpha, beta, gamma, etc.), energy, and target. Consequently, photons entering any shielding will be attenuated by scattering within that material. In realistic cases, we quantify the attenuation of a photon beam (I_0) transmitted through any material having a thickness x and a linear attenuation coefficient μ using the modified Beer–Lambert law [2, 3]:

$$I = BI_0e^{-\mu x}. \quad (1)$$

The correction parameter B (called the buildup factor) was introduced because of violations of the Beer–Lambert law, which assumes monochromatic rays, thin shielding, and a narrow beam geometry. There are mainly two types:

This work was supported by the National Plan for Science, Technology and Innovation (MAARIFAH), King Abdulaziz City for Science and Technology, Kingdom of Saudi Arabia, Award Number (12-MED2516-02).

Electronic supplementary material The online version of this article (<https://doi.org/10.1007/s41365-019-0701-4>) contains supplementary material, which is available to authorized users.

✉ O. Kadri
okadri@cern.ch

¹ Department of Radiological Sciences, College of Applied Medical Sciences, King Saud University, PO Box 10219, Riyadh 11433, Saudi Arabia

² National Center for Nuclear Sciences and Technologies, 2020 Tunis, Tunisia

the exposure and energy absorption buildup factors (EBF and EABF), which refer to the energy deposited in air and in the attenuating material, respectively. The precise gamma-ray EABF and EBF are generally not easy to measure experimentally. Therefore, studies of gamma-ray buildup factors were carried out using Monte Carlo simulation [4], invariant embedding [5], geometric progression (GP) fitting [6–8], and other methods. However, on the basis of our knowledge and the available literature, there is no more precise dataset of buildup factors than those tabulated by ANSI/ANS-6.4.3-1991 [9]. This dataset provides five GP fitting parameters for 23 elements and three compounds in an energy range of 0.015–15 MeV at penetration depths up to 40 mean free paths (mfp) for both buildup factors. Many buildup factors for different types of materials have been successfully calculated using various computation methods. However, a unified dataset for all human body tissues and for deep penetration (up to 100 mfp) can be considered valuable to the scientific research community, as it could be straightforwardly included in point kernel-based programs. Moreover, the GEometry ANd Tracking version 4 (Geant4) Monte Carlo toolkit [10, 11] has not been used to fully simulate buildup factors, except for recently published work in which the mass energy attenuation coefficients were simulated and used with the GP parameters [2].

In order to address the questions outlined above, we propose a framework for computing the EABF and EBF values of point isotropic sources for deep penetration of selected materials. GP fitting and Monte Carlo simulation methods are used to compute the buildup factors for 30 human body tissues representing the full material needs for point kernel calculation applied to the High-Definition Reference Korean-Man (HDRK-Man) [12–14]. Our goal can be summarized as follows: (i) verification of the calculation method against standards, (ii) study of the buildup factor-dependent parameters, and (iii) investigation of some tissue substitute materials. Thus, after calculating the GP fitting parameters using the XCOM data for all elements ($Z = 4–92$) for 25 standard photon energies (0.015–15 MeV) [15], we first carried out a rapid checkout of the EABF and EBF of water for selected penetration depths (1, 20, 40, 80, and 100 mfp) and compared them to ANSI/ANS-6.4.3-1991 data. Then, we examined the effects of the energy, equivalent atomic number (Z_{eq}), and penetration depth on both buildup factors and compared them to each other. In addition, we investigated the applicability of the method to materials commonly used to replace human tissues by comparing Z_{eq} as a function of energy for three types of tissues (adipose tissue, lung, and skeletal muscle) against three materials (AP6, LN1, and M3, respectively) [16]. Finally, a Geant4 Monte Carlo simulation of the full

setup was carried out to compute the EABF of water for a photon energy of 0.1 MeV and penetration depths up to 10 mfp, and the results were compared to data extracted from the literature. Consequently, this paper may be of great interest to radiation physics researchers and can be considered as a continuation of therapeutic and diagnostic research, other than shielding purposes.

2 Materials and methods

In the following subsections, we describe in detail the procedures used for the GP fitting and Monte Carlo simulation techniques.

2.1 GP fitting method

To calculate the buildup factors, the GP fitting parameters were obtained by interpolation from the equivalent atomic number (Z_{eq}). The computational work was carried out as follows:

- Calculation of the equivalent atomic number, Z_{eq}
- Calculation of GP fitting parameters
- Calculation of energy absorption and exposure buildup factors

2.1.1 Calculation of the equivalent atomic number (Z_{eq})

The equivalent atomic number, Z_{eq} , is an energy-dependent parameter describing the properties of a composite material in terms of equivalent elements. We started by extracting the Compton partial mass attenuation coefficient $(\mu/\rho)_{\text{Compton}}$ and total mass attenuation coefficient $(\mu/\rho)_{\text{Total}}$ for all elements with $Z = 4–92$ and for the chosen dosimetric materials in an energy range of 0.015–15 MeV using the WinXCom computer program [17] (initially developed as XCOM). Then, to interpolate Z_{eq} when the ratio $(\mu/\rho)_{\text{Compton}}/(\mu/\rho)_{\text{Total}}$ for a given human organ or tissue lies between two successive ratios of elements, the following formula was employed [18]:

$$Z_{\text{eq}} = \frac{Z_1(\log R_2 - \log R) + Z_2(\log R - \log R_1)}{\log R_2 - \log R_1}, \quad (2)$$

where Z_1 and Z_2 are the atomic numbers of the two elements, R_1 and R_2 are the ratios $(\mu/\rho)_{\text{Compton}}/(\mu/\rho)_{\text{Total}}$ for these elements, and R is the corresponding ratio for a given human organ or tissue at a given energy that lies between R_1 and R_2 (the nearest neighbors of R).

2.1.2 Calculation of the GP fitting parameters

Taking the GP fitting parameters for pure elements from the standard reference, ANSI/ANS-6.4.3-1991, and using the previously calculated Z_{eq} , we interpolated the corresponding GP fitting parameters ($a, b, c, d,$ and X_k) for the buildup factors using the following formula [19–21]:

$$P = \frac{P_1(\log Z_2 - \log Z_{eq}) + P_2(\log Z_{eq} - \log Z_1)}{\log Z_2 - \log Z_1}, \tag{3}$$

where $P, P_1,$ and P_2 refer to the same GP parameters for the selected organ or tissue and both neighbors (which correspond to Z_1 and Z_2).

2.1.3 Calculation of the buildup factors

For a given photon energy and shielding material, we used two different sets of GP parameters to calculate the EABF and EBF. Thus, we first tabulated all the parameters from ANS-6.4.3-1991 and proceeded to calculate the buildup factors for a given incident photon energy E and penetration depth (source–detector distance) x , in mfp, as follows [2, 6, 22–24]:

$$B(E, x) = 1 + (b - 1) \times \begin{cases} x & \text{if } K = 1 \\ \frac{K^x - 1}{K - 1} & \text{if } K \neq 1 \end{cases} \tag{4}$$

where for $x \leq 40$ mfp:

$$K(E, x) = cx^a + d \frac{\tanh(x/X_k - 2) - \tanh(-2)}{1 - \tanh(-2)} \tag{5}$$

and for $x \geq 40$ mfp:

$$K(E, x) = \begin{cases} 1 + (K_{35} - 1)\Phi^{\xi(x)} & \text{if } 0 \leq \Phi \leq 1 \\ K_{35} \left(\frac{K_{40}}{K_{35}}\right)^{0.8\xi(x)} & \text{otherwise} \end{cases} \tag{6}$$

where $\Phi = \frac{K_{40}-1}{K_{35}-1}$, $\xi(x) = \frac{(x/35)^{0.1}-1}{(40/35)^{0.1}-1}$, $K_{35} = K(E, 35)$, and $K_{40} = K(E, 40)$. For deep penetration (greater than 40 mfp), an extrapolation of the dose multiplication factor $K(E, x)$ was proposed by Harima et al. [23] and supported by Sakamoto and Trubey [25].

2.2 Geant4 simulation method

Geant4 is a Monte Carlo simulation toolkit developed and managed mainly by the European Center for Nuclear Research for modeling and simulation of fermion, boson, hadron, ion, and hypothetical and short-lived particle transport. It was used to indirectly benchmark ANSI data by computing mass attenuation coefficients and using GP fitting parameters [2]. By contrast, this is the first attempt to use Geant4 to directly compute the buildup factors. Here,

we studied only water as a material to avoid simulation run-time penalties and because of its overall similarity, in terms of chemical composition, to human organ materials. Further, a successful benchmark will allow us to extend the simulation to all human organs and tissues when the necessary hardware is available. This topic will be investigated in our next work. In this study, Geant4 version 10.4 was used to simulate the transport of gamma rays emitted from a point source through water. The geometry of the problem consists of a monoenergetic point source located at the center of concentric spheres. We simulated the transport of photons with an energy of 0.1 MeV isotropically generated from the center of an infinite sphere with an outer radius of 105.45 cm (which is equivalent to 18 mfp). Using the energy flux to exposure conversion factors provided in the literature [26], we converted the simulated exit flux (for each step of 1 mfp) to the EBF using the mass energy absorption coefficient of air obtained from the NIST Web site [27]. We calculated the EBF of water for a photon energy of 0.1 MeV and penetration depths up to 10 mfp. In this study, the buildup factor was computed for 10^8 gamma rays. We deactivated the bremsstrahlung and activated all the other processes for electrons and photons. We used the G4EmStandardPhysics_option3 built-in physics library and used a 1 keV cutoff for electrons and photons. The overall statistical uncertainty did not exceed 1% in any simulation.

3 Results and discussion

We calculated Z_{eq} , the GP fitting parameters, the EABF, and the EBF for 30 types of tissue (see Table 1 for the elemental compositions) of the HDRK-Man human phantom and for five mixtures: water, air, AP6, LN1, and M3. All the results are tabulated in Annex (Supplementary data).

3.1 Standardization of the calculation method

Figure 1 shows the computed values of the EABF and EBF for water for penetration depths of 1, 20, 40, 80, and 100 mfp and photon energies in a range of 0.015–15 MeV. For comparison, the results are plotted together with standard values (up to 40 mfp) provided by ANSI/ANS 6.4.3-1991. The EBF values were also compared, when available, to the data of Harima et al. [28] for a penetration depth of 100 mfp. Further, we compared the EABFs calculated in this work for blood and adipose tissue as a function of photon energy at a penetration depth of 40 mfp to those of Manohara et al. [21] and Olarinoye [24]. Table 2 shows that our results deviate by 3.75 ± 2.07 and

Table 1 Elemental composition (%) of studied HDRK-Man organs/tissues and phantom materials

Material	H	C	N	O	Na	P	S	Cl	K	Other
Water	11.11			88.89						
Air		0.01	75.53	23.78						Ar (1.28)
AP6	8.36	69.14	2.36	16.94				0.14		F (3.07)
LN1	6.00	51.44	4.29	30.72						Al (7.55)
M3	11.43		65.58		9.22					Mg (13.48), Ca (0.29)
RBM	10.50	41.40	3.40	43.90		0.10	0.20	0.20	0.20	Fe (0.10)
Colon	10.60	11.50	2.20	75.10	0.10	0.10	0.10	0.20	0.10	
Lung	10.13	10.24	2.87	75.75	0.18	0.08	0.22	0.27	0.19	Ca (0.01), Fe (0.04) Zn (<0.01), Rb (<0.01)
Stomach	10.60	11.50	2.20	75.10	0.10	0.10	0.10	0.20	0.10	
Breast	11.40	59.80	0.70	27.80	0.10		0.10	0.10		
Gonads (testis)	10.60	9.90	2.00	76.60	0.20	0.10	0.20	0.20	0.20	
Bladder	10.50	9.60	2.60	76.10	0.20	0.20	0.20	0.30	0.30	
Esophagus	10.50	25.60	2.70	60.20	0.10	0.20	0.30	0.20	0.20	
Liver	10.20	13.90	3.00	71.60	0.20	0.30	0.30	0.20	0.30	
Thyroid	10.40	11.90	2.40	74.50	0.20	0.10	0.10	0.20	0.10	I (0.10)
Bone	7.34	25.47	3.06	47.89	0.33	5.09	0.17	0.14	0.15	F (0.02), Mg (0.11) Si (0.02), Ca (10.19) Fe (0.01), Zn (<0.01) Rb (<0.01), Sr (<0.01) Pb (<0.01)
Brain	10.70	14.50	2.20	71.20	0.20	0.40	0.20	0.30	0.30	
Salivary glands	10.50	25.60	2.70	60.20	0.10	0.20	0.30	0.20		
Skin	10.00	20.40	4.20	64.50	0.20	0.10	0.20	0.30		
Adrenal	10.50	25.60	2.70	60.20	0.10	0.20	0.30	0.20	0.20	
ET	10.50	25.60	2.70	60.20	0.10	0.20	0.30	0.20	0.20	
Gall bladder	10.50	25.60	2.70	60.20	0.10	0.20	0.30	0.20	0.20	
Heart	10.40	13.90	2.90	71.80	0.10	0.20	0.20	0.20	0.30	
Kidneys	10.30	13.20	3.00	72.40	0.20	0.20	0.20	0.20	0.20	Ca (0.10)
Blood	10.20	11.00	3.30	74.50	0.10	0.10	0.20	0.30	0.20	Fe (0.10)
Muscle	10.20	14.30	3.40	71.00	0.10	0.20	0.30	0.10	0.40	
Oral mucosa	8.43	57.40	1.61	24.55				0.13		Mg (7.88)
Pancreas	10.60	16.90	2.20	69.40	0.20	0.20	0.10	0.20	0.20	
Prostate	10.50	25.60	2.70	60.20	0.10	0.20	0.30	0.20	0.20	
Intestine	10.60	11.50	2.20	75.10	0.10	0.10	0.10	0.20	0.10	
Spleen	10.30	11.30	3.20	74.10	0.10	0.30	0.20	0.20	0.30	
Thymus	10.50	25.60	2.70	60.20	0.10	0.20	0.30	0.20	0.20	
Eyes	9.60	19.50	5.70	64.60	0.10	0.10	0.30	0.10		
Lens	9.60	19.50	5.70	64.60	0.10	0.10	0.30	0.10		
Adipose tissue	11.40	59.80	0.70	27.80	0.10		0.10	0.10		

4.57 ± 3.00 for blood and by 2.74 ± 2.45 and 3.89 ± 2.62 for adipose tissue from those reported by Manohara et al. and Olarinoye, respectively. The good agreement seen in the plots and tabulated data enable us to safely proceed with the present method of calculating the buildup factors for other media such as human body tissues and organs.

3.2 Energy absorption and exposure buildup factors

The GP fitting parameters for the 30 human organs and tissues computed using the procedure described above were used to generate the EABFs and EBFs. The computed Z_{eq} , GP fitting parameters, EABFs, and EBFs are tabulated in

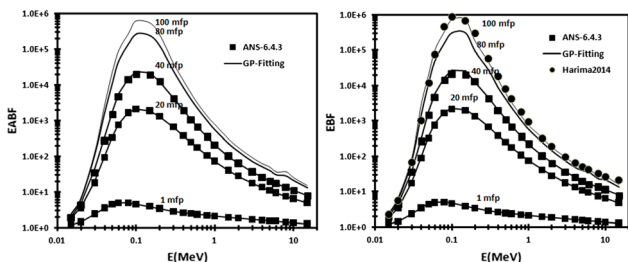


Fig. 1 Calculated energy absorption and EBFs of water as a function of photon energy compared to ANSI/ANS-6.4.3 and data of Harima et al. [28] for penetration depths up to 100 mfp

Annex (Supplementary data) for all the studied materials at 25 standard photon energies (0.015–15 MeV) and 17 standard penetration depths (1–100 mfp). In the following subsections, we evaluate the buildup factors’ dependence on the incident photon energy, chemical composition, and penetration depth.

3.2.1 Incident photon energy dependence

Figure 1 shows the energy dependence of the buildup factors at selected penetration depths from 1 to 100 mfp for water. All the human tissues and organs behaved similar to water [as shown in Table 2 and Annex (Supplementary data)] owing to their similarity in terms of chemical composition (the major elements are H, C, N, O, Na, P, S, Cl, and K, as shown in Table 1). For all the plots, the buildup factor curves increased to a maximum value and then decreased more slowly. This fact confirms the predictions from theory and the literature, as the dominance of the photoelectric effect increased from a low energy up to a specific energy at which it equals the Compton effect, namely E_{pe} . Moreover, if E_{pp} is the energy at which the Compton and pair production cross sections are equal, the buildup factors reach their maximum at an energy

Table 2 Calculated EABF values for blood and adipose tissue as a function of energy for a penetration depth of 40 mfp

E (MeV)	Blood					Adipose tissue				
	This work	Manohara	Olarinoye	Δ_1	Δ_2	This work	Manohara	Olarinoye	Δ_1	Δ_2
1.5E-2	1.97E+0	1.83E+0	1.94E+0	7.59E+0	1.35E+0	3.14E+0	3.03E+0	3.15E+0	3.72E+0	2.73E-3
2.0E-2	4.32E+0	4.36E+0	3.97E+0	8.82E-1	8.67E+0	1.18E+1	1.15E+1	1.23E+1	3.24E+0	3.74E+0
3.0E-2	3.87E+1	3.77E+1	3.76E+1	2.77E+0	2.87E+0	1.96E+2	1.97E+2	1.84E+2	5.02E-1	6.23E+0
4.0E-2	2.57E+2	2.66E+2	2.53E+2	3.57E+0	1.68E+0	2.42E+3	2.45E+3	2.34E+3	9.52E-1	3.62E+0
5.0E-2	1.33E+3	1.42E+3	1.32E+3	6.24E+0	5.60E-1	1.10E+4	1.09E+4	1.09E+4	1.02E+0	1.21E+0
6.0E-2	4.06E+3	4.05E+3	4.03E+3	2.80E-1	9.20E-1	2.54E+4	2.59E+4	2.58E+4	1.94E+0	1.53E+0
8.0E-2	1.17E+4	1.20E+4	1.08E+4	2.86E+0	8.19E+0	4.72E+4	4.94E+4	4.50E+4	4.39E+0	4.89E+0
1.0E-1	1.76E+4	1.73E+4	1.68E+4	1.68E+0	4.47E+0	5.74E+4	5.69E+4	5.78E+4	8.80E-1	7.17E-1
1.5E-1	1.72E+4	1.63E+4	1.68E+4	5.29E+0	2.26E+0	3.48E+4	3.50E+4	3.29E+4	6.54E-1	5.70E+0
2.0E-1	1.05E+4	1.07E+4	9.94E+3	1.68E+0	5.48E+0	1.78E+4	1.73E+4	1.78E+4	2.89E+0	1.96E-1
3.0E-1	3.96E+3	4.05E+3	3.87E+3	2.39E+0	2.34E+0	5.19E+3	5.16E+3	4.90E+3	4.57E-1	5.83E+0
4.0E-1	1.85E+3	1.85E+3	1.75E+3	4.68E-1	6.26E+0	2.26E+3	2.17E+3	2.11E+3	4.00E+0	6.70E+0
5.0E-1	1.04E+3	1.09E+3	9.85E+2	4.58E+0	5.86E+0	1.23E+3	1.21E+3	1.24E+3	1.86E+0	8.12E-1
6.0E-1	6.63E+2	7.01E+2	6.14E+2	5.44E+0	7.95E+0	7.28E+2	6.87E+2	7.09E+2	5.90E+0	2.69E+0
8.0E-1	3.43E+2	3.33E+2	3.14E+2	3.07E+0	9.19E+0	3.49E+2	3.33E+2	3.23E+2	5.07E+0	8.06E+0
1.0E+0	2.11E+2	2.01E+2	2.01E+2	5.16E+0	5.33E+0	2.19E+2	2.01E+2	2.01E+2	9.09E+0	9.17E+0
1.5E+0	1.00E+2	9.72E+1	9.74E+1	2.91E+0	2.69E+0	1.00E+2	9.34E+1	9.68E+1	7.36E+0	3.57E+0
2.0E+0	6.34E+1	5.99E+1	5.92E+1	5.80E+0	7.08E+0	6.36E+1	5.99E+1	6.35E+1	6.10E+0	1.11E-1
3.0E+0	3.65E+1	3.41E+1	3.34E+1	6.99E+0	9.27E+0	3.59E+1	3.48E+1	3.33E+1	3.35E+0	7.93E+0
4.0E+0	2.59E+1	2.52E+1	2.41E+1	2.71E+0	7.26E+0	2.54E+1	2.57E+1	2.51E+1	1.08E+0	1.17E+0
5.0E+0	2.07E+1	1.94E+1	1.92E+1	6.89E+0	7.58E+0	2.02E+1	1.98E+1	1.95E+1	2.05E+0	3.44E+0
6.0E+0	1.74E+1	1.68E+1	1.78E+1	3.15E+0	2.74E+0	1.72E+1	1.72E+1	1.65E+1	4.76E-1	4.74E+0
8.0E+0	1.39E+1	1.32E+1	1.39E+1	5.23E+0	7.0E-2	1.38E+1	1.38E+1	1.31E+1	8.29E-2	4.73E+0
1.0E+1	1.13E+1	1.10E+1	1.17E+1	2.62E+0	2.96E+0	1.10E+1	1.10E+1	1.08E+1	4.19E-1	1.68E+0
1.5E+1	8.10E+0	7.82E+0	8.20E+0	3.58E+0	1.28E+0	7.90E+0	7.98E+0	7.69E+0	9.60E-1	2.74E+0

Comparisons with other works (Manohara et al. [21] and Olarinoye [24]) are provided, with the corresponding deviations (in %) (Δ_1 and Δ_2 for [21] and [24], respectively)

$E_{pe} \leq E \leq E_{pp}$, because Compton scattering results in more multiply scattered photons.

3.2.2 Equivalent atomic number dependence

Figure 2 shows the buildup factor values as a function of Z_{eq} for some tissues and organs at photon energies of 0.015, 0.15, 1.5, and 15 MeV and penetration depths of 5, 40, and 100 mfp. This figure demonstrates that the buildup factors were inversely proportional to Z_{eq} at photon energies of 0.015 and 0.15 MeV and independent of Z_{eq} at 1.5 and 15 MeV for all penetration depths. Thus, for low-energy photons, the buildup factor decreased with increasing Z_{eq} (chemical compounds), whereas for high-energy photons, it remained insensitive to the chemical composition of the

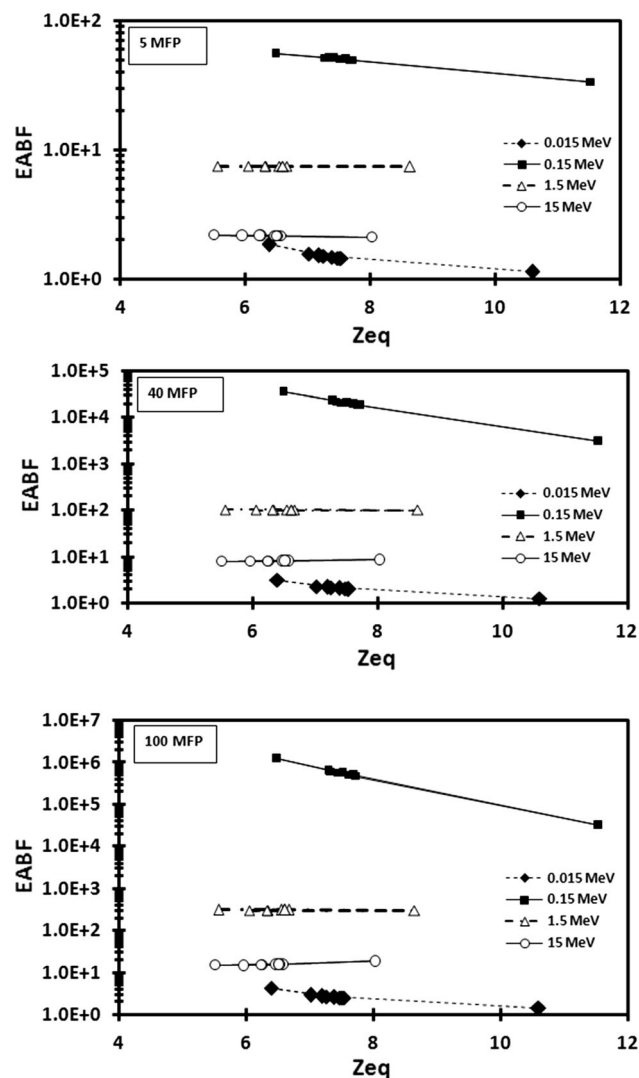


Fig. 2 Calculated EABF of Z_{eq} for photon energies of 0.015, 0.15, 1.5, and 15 MeV and penetration depths of 5, 40, and 100 mfp for studied tissues

medium. Here, we confirmed the conclusions reported elsewhere [2, 18, 21, 24, 29].

In addition, we calculated and plotted Z_{eq} as a function of photon energy for the standard grid for some tissue substitutes commonly used in experimental radiation physics [16]. Figure 3 shows that the chemical compositions of the three tissues (adipose, lung, and muscle tissue) are equivalent to those of their substitute materials (AP6, LN1, and M3, respectively), especially at lower energies (up to 1 MeV). However, we see that M3 cannot be used as a muscle substitute, and AP6 can replace adipose tissue moderately well, at higher energies (above 1 MeV). This can be explained by the fact that the pair production effect is proportional to the square of the atomic number. In Table 1, the difference in elemental composition between M3 and muscle tissue is clear, and that between AP6 and adipose tissue is moderately clear.

3.2.3 Penetration depth dependence

From the plots of EABF as a function of penetration depth for selected tissues in Fig. 4, it can be seen that at a lower energy of 0.015 MeV, bone and breast have the lowest and highest buildup factors, respectively, for penetration depths up to 100 mfp. This effect can be explained by the differences in chemical composition of different tissues, as adipose tissue and bone have Z_{eq} values of 6.389 and 10.59, respectively. Further, at a photon energy of 0.15 MeV, the buildup values become more similar until they coincide to form a single dataset at a photon energy of 1.5 MeV for all penetration depths. Table 3 illustrates the good agreement between our results and those of Olarinoye for

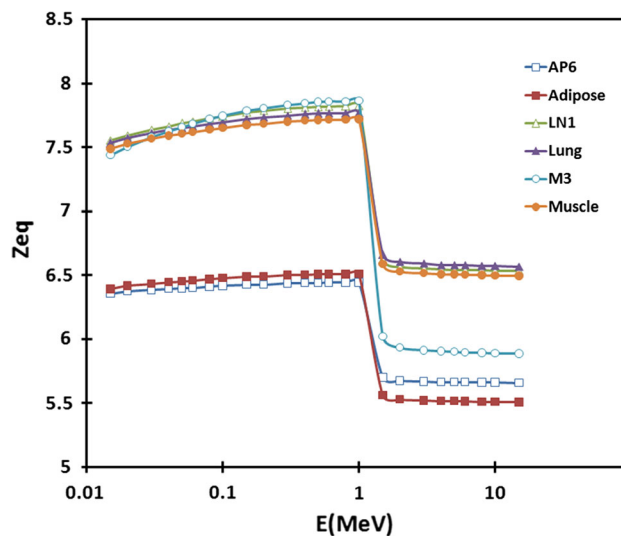


Fig. 3 Z_{eq} values of some tissues (adipose tissue, lung, muscle) and their substitutes (AP6, LN1, M3, respectively) as a function of photon energy

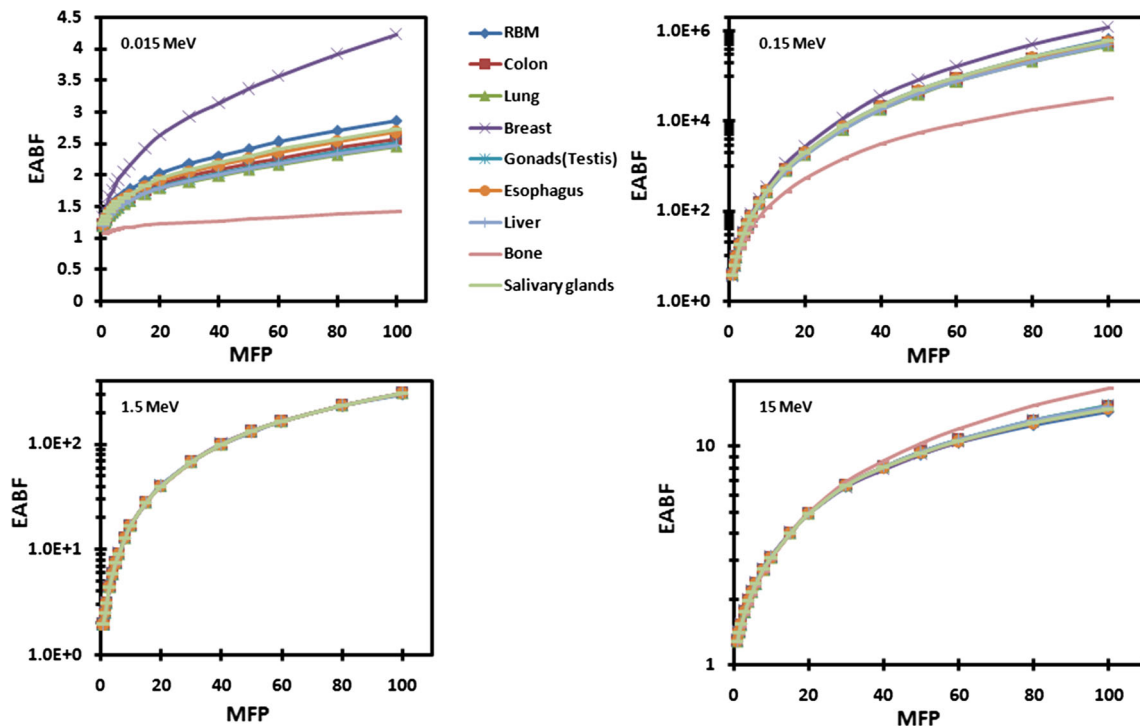


Fig. 4 Variation in the EABF of the penetration depth for selected human tissues at various photon energies

two human tissues for deep penetration (up to 100 mfp). Moreover, at a photon energy of 15 MeV, all the tissues have equal buildup values up to 20 mfp, where the data for bone tissue alone started to increase up to 100 mfp, and all the other tissues continued to exhibit similar behavior. In addition, the higher magnitude of the buildup factors at a photon energy of 0.15 MeV compared to the other cases can be explained by the important increase in multiply scattered photons, remembering that the buildup factor was defined as the ratio of scattered to primary photons.

3.2.4 Comparison of EABF and EBF

Figure 5 shows a comparison of the buildup factors for breast (adipose) and bone tissues at photon energies of 0.015–15 MeV and selected penetration depths of 1, 20, 40, and 80 mfp. The plotted ratios of the EABF and EBF indicate that they are equivalent for both materials at low energies (≤ 40 keV) and high energies (≥ 3 MeV). However, at an intermediate energy, we can see that the EABF was lower than the EBF for breast tissue and higher than the EBF for bone tissue at all penetration depths. This

Table 3 Calculated EABF values for blood and adipose tissues as a function of penetration depth for photon energy of 0.015 MeV

MFP	Blood			Adipose tissue		
	This work	Olarinoye	Δ_1	This work	Olarinoye	Δ_1
1	1.19E+0	1.19E+0	1.36E-1	1.33E+0	1.33E+0	3.60E-1
1.5	1.44E+0	1.47E+0	2.52E+0	1.85E+0	1.84E+0	2.33E-1
10	1.58E+0	1.60E+0	1.01E+0	2.17E+0	2.17E+0	4.30E-2
15	1.69E+0	1.70E+0	4.44E-1	2.42E+0	2.43E+0	4.06E-1
20	1.77E+0	1.78E+0	1.91E-1	2.63E+0	2.64E+0	1.99E-1
30	1.88E+0	1.88E+0	1.49E-1	2.92E+0	2.92E+0	3.70E-2
40	1.97E+0	1.94E+0	1.35E+0	3.14E+0	3.15E+0	2.73E-1
50	2.06E+0	2.06E+0	5.60E-2	3.36E+0	3.38E+0	5.36E-1
60	2.15E+0	2.14E+0	1.64E-1	3.56E+0	3.59E+0	8.57E-1
80	2.30E+0	2.30E+0	4.30E-2	3.92E+0	3.95E+0	8.70E-1
100	2.43E+0	2.43E+0	2.53E-1	4.23E+0	4.25E+0	3.83E-1

Comparison to other work (Olarinoye [24]) is shown with the corresponding deviation (Δ_1 , in %)

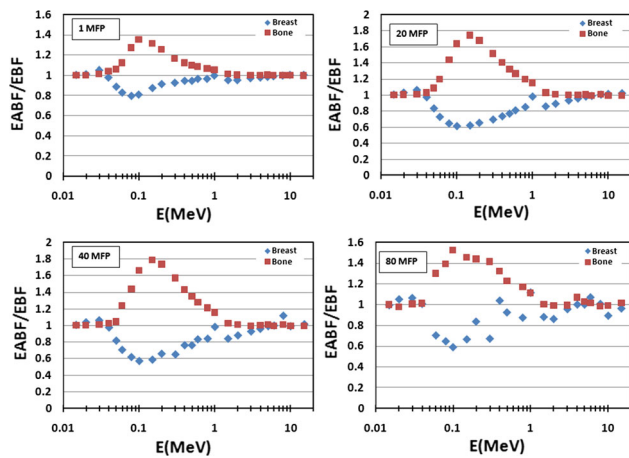


Fig. 5 Comparison of EABF and EBF for breast and bone tissues as a function of photon energy for selected penetration depths

behavior confirms the theory of gamma-ray exposure in air and media. It can be explained by comparing their Z_{eq} values to that of air, as the equivalent number for air was greater than Z_{eq} for breast tissue and lower than Z_{eq} for bone tissue in the entire studied energy range.

3.2.5 Geant4 benchmark

We compared our results to those published in the literature [30] for the EBF of water for a point isotropic source of photons with an energy of 0.1 MeV and penetration depths up to 10 mfp. Figure 6 shows that the current computations are in good agreement with the literature. During our simulations, we followed the energy discrimination method with an energy window (ϵ) of 10%, as described elsewhere [29]. This method assumed that a gamma ray having an energy between E_0 and $E_0 - \epsilon$ can be considered to be uncollided; otherwise, it will be counted as collided. However, the small discrepancies observed, especially for deeper penetration, can be corrected either by using a supercomputer (not laptops, as in our study) or by using particle splitting as a variance reduction technique [30, 31]. These phenomena can be explained by the decrease in photon detection probability at large distances from the source.

4 Conclusion

Recent estimations of the transport and degradation of gamma rays in human tissues have provided a dataset of the EBFs and EABFs. The current findings represent a valuable extension of the buildup factor calculation and simulation for 30 tissues/organs (describing all materials used in the HDRK-Man phantom) and five compounds, for

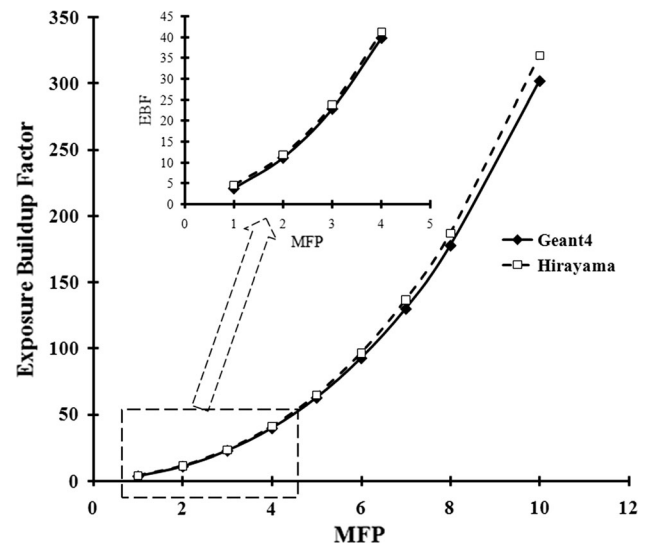


Fig. 6 Geant4-simulated EBF of water (for 0.1 MeV photons) as a function of penetration depth compared to data extracted from the work of Hirayama [30]

a point isotropic source of photons with energies of 0.015–15 MeV and for deep penetration (up to 100 mfp). The results of a Geant4 simulation suggested that the use of a variance reduction technique (i.e., particle splitting) will yield better accuracy for deep penetration. Moreover, the results of the GP fitting method demonstrated that the buildup factors reached their maxima for photon energies of $E_{pe} \leq E \leq E_{pp}$ and that they were inversely proportional to Z_{eq} for $E \leq 0.15$ MeV and independent of Z_{eq} for $E \geq 1.5$ MeV for all penetration depths. A comparison of the EABFs to the EBFs allowed us to conclude that at low energies (≤ 40 keV) and high energies (≥ 3 MeV), they behave similarly. (Their ratio was close to one.) Nevertheless, at intermediate energies, any material having a Z_{eq} value lower than that of air has $EABF \leq EBF$ for all penetration depths. Additionally, materials with a Z_{eq} exceeding that of air are characterized by $EABF \geq EBF$ for all penetration depths and for intermediate photon energies. In addition, we confirmed previously reported results on the effect of penetration depth on the buildup factors and extended them to penetration depths of more than 40 mfp (up to 100 mfp), demonstrating that at a photon energy of 1.5 MeV, the factors were independent of the chemical composition of the medium. Further similar work can be performed using the GP fitting and Geant4 simulation methods for multilayer shielding, plane parallel sources, and neutron particles. The present work can be considered as extending knowledge regarding radiation protection guidelines.

References

1. F.O. Ogundare, I.O. Olarinoye, R.I. Obed., Estimation of patients' organ and conceptus doses from selected x-ray examinations in two Nigeria x-ray centers. *Radiat. Prot. Dosim.* **132**(4), 395–402 (2009). <https://doi.org/10.1093/rpd/ncn317>
2. K.S. Mann, T. Korkut, Gamma-ray buildup factors study for deep penetration in some silicates. *Ann. Nucl. Energy* **51**, 81–93 (2013). <https://doi.org/10.1016/j.anucene.2012.08.024>
3. S.P. Singh, T. Singh, P. Kaur, Variation of energy absorption buildup factors with incident photon energy and penetration depth for some commonly used solvents. *Ann. Nucl. Energy* **35**, 1093–1097 (2008). <https://doi.org/10.1016/j.anucene.2007.10.007>
4. D. Sardari, A. Abbaspour, S. Baradaran et al., Estimation of gamma- and X-ray photons buildup factor in soft tissue with Monte Carlo method. *Appl. Radiat. Isot.* **67**, 1438–1440 (2009). <https://doi.org/10.1016/j.apradiso.2009.02.033>
5. A. Shimizu, H. Hirayama, Calculation of gamma-ray buildup factors up to depths of 100 mfp by the method of invariant embedding. (II) improved treatment of bremsstrahlung. *J. Nucl. Sci. Technol.* **40**, 192–200 (2003). <https://doi.org/10.3327/jnst.40.192>
6. Y. Harima, Y. Sakamoto, S. Tanaka et al., Validity of the geometric progression formula in approximating gamma ray buildup factors. *Nucl. Sci. Eng.* **94**, 24–35 (1986). <https://doi.org/10.13182/NSE86-A17113>
7. M. Kurudirek, Y. Kurucu, Estimation of energy absorption buildup factors of some human tissues at energies relevant to brachytherapy and external beam radiotherapy. *Int. J. Radiat. Biol. Sep* **17**, 1–27 (2019). <https://doi.org/10.1080/09553002.2019.1665217>
8. B. Mehmet, M. Kurudirek, Radiological properties of healthy, carcinoma and equivalent breast tissues for photon and charged particle interactions. *Int. J. Radiat. Biol.* **94**(1), 70–78 (2018). <https://doi.org/10.1080/09553002.2018.1403057>
9. American Nuclear Society, *Gamma Ray Attenuation Coefficient and Buildup Factors for Engineering Materials*. Report ANSI/ANS-6.4.3, USA (1991)
10. S. Agostinelli, J. Allison, K. Amako et al., Geant4-a simulation toolkit. *NIMA* **506**(3), 250–303 (2003). [https://doi.org/10.1016/S0168-9002\(03\)01368-8](https://doi.org/10.1016/S0168-9002(03)01368-8)
11. J. Allison, K. Amako, J. Apostolakis et al., Recent developments in Geant4. *NIMA* **835**(1), 186–225 (2016). <https://doi.org/10.1016/j.nima.2016.06.125>
12. C.H. Kim, S.H. Choi, J.H. Jeong et al., HDRK-Man: a whole-body voxel model based on high-resolution color slice images of a Korean adult male cadaver. *Phys. Med. Biol.* **53**(15), 4093–4106 (2008). <https://doi.org/10.1088/0031-9155/53/15/006>
13. A. Alfuraih, O. Kadri, K. Alzimami, Investigation of SPECT/CT cardiac imaging using Geant4. *Nucl. Sci. Tech.* **29**, 7 (2018). <https://doi.org/10.1007/s41365-018-0435-8>
14. O. Kadri, K. Manai, A. Alfuraih, Monte Carlo study of the cardiac absorbed dose during x-ray examination of an adult patient. *Radiat. Prot. Dosim.* **171**(4), 431–437 (2016). <https://doi.org/10.1093/rpd/ncv429>
15. M.J. Berger, J.H. Hubbell, *XCOM: Photon Cross Sections on a Personal Computer*. NBSIR 87-3597 (National Bureau of Standards, Washington, 1987). <https://doi.org/10.2172/6016002>
16. D.R. White, Tissue substitutes in experimental radiation physics. *Med. Phys.* **5**(6), 467–479 (1978). <https://doi.org/10.1118/1.594456>
17. L. Gerward, N. Guilbert, K.B. Jensen et al., WinXCom: a program for calculating x-ray attenuation coefficients. *Radiat. Phys. Chem.* **71**, 653–654 (2004). <https://doi.org/10.1016/j.radphyschem.2004.04.040>
18. M. Kurudirek, Y. Ozdemir, Energy absorption and exposure buildup factors for some polymers and tissue substitute materials: photon energy, penetration depth and chemical composition dependence. *J. Radiol. Prot.* **31**, 117–128 (2011). <https://doi.org/10.1088/0952-4746/31/1/008>
19. Y. Harima, An approximation of gamma-ray buildup factors by modified geometrical progression. *Nucl. Sci. Eng.* **83**(2), 299–309 (1983). <https://doi.org/10.13182/NSE83-A18222>
20. M.J. Maron, *Numerical Analysis: A Practical Approach* (Macmillan, New York, 1987)
21. S.R. Manohara, S.M. Hanagodimath, L. Gerward, Energy absorption buildup factors of human organs and tissues at energies and penetration depths relevant for radiotherapy and diagnostics. *J. Appl. Clin. Med. Phys.* **12**(4), 296–312 (2011). <https://doi.org/10.1120/jacmp.v12i4.3557>
22. V.P. Singh, M.E. Medhat, N.M. Badiger, Assessment of exposure buildup factors of some oxide dispersion strengthened steels applied in modern nuclear engineering and designs. *Nucl. Eng. Des.* **270**, 90–100 (2014). <https://doi.org/10.1016/j.nucengdes.2013.12.046>
23. Y. Harima, S. Tanaka, Y. Sakamoto et al., Development of new gamma-ray buildup factor and application of shielding calculations. *Nucl. Sci. Eng.* **94**, 24–35 (1991)
24. I.O. Olarinoye, Photon buildup factors for some tissues and phantom materials for penetration depths up to 100 MFP. *J. Nucl. Res. Dev.* **13**, 57–67 (2017)
25. Y. Sakamoto, D.K. Trubey, *Radiation Safety Information Computation Center Data Package DLC-129/ANS643, Geometric Progression*. Gamma-Ray Buildup Factor Coefficients (1991)
26. J.H. Smith, *Flux to Dose Rate Conversion Factors for Gamma Ray Exposure*. JPL technical report, no. 32-439 (1963)
27. <https://www.nist.gov/pml/x-ray-mass-attenuation-coefficients>. Accessed 27 Aug 2019
28. Y. Harima, N. Kurosawa, Y. Sakamoto, Parameter search of geometric-progression formula for gamma-ray isotropic point source buildup factors up to depths of 100 mfp, including contribution of secondary radiations. *Progr. Nucl. Sci. Technol.* **4**, 548–552 (2014). <https://doi.org/10.15669/pnst.4.548>
29. I. Jarrah, M.I. Radaideh, T. Kozlowski et al., Determination and validation of photon energy absorption buildup factor in human tissues using Monte Carlo simulation. *Radiat. Phys. Chem.* **160**, 15–25 (2019). <https://doi.org/10.1016/j.radphyschem.2019.03.008>
30. H.J. Hirayama, Calculation of gamma-ray exposure buildup factors up to 40 mfp using the EGS4 Monte Carlo code with a particle splitting. *J. Nucl. Sci. Technol.* **32**(12), 1201–1207 (1995). <https://doi.org/10.3327/jnst.32.1201>
31. M.M. Rafiei, H. Tavakoli-Anbaran, Calculation of the exposure buildup factors for x-ray photons with continuous energy spectrum using Monte Carlo code. *J. Radiol. Prot.* **38**, 207 (2018). <https://doi.org/10.1088/1361-6498/aa9cfa>